Copolymerization of 2-Carboxyisopropylacrylamide with *N*-Isopropylacrylamide Accelerates Cell Detachment from Grafted Surfaces by Reducing Temperature

Mitsuhiro Ebara,† Masayuki Yamato,‡ Motohiro Hirose,‡ Takao Aoyagi,‡ Akihiko Kikuchi,‡ Kiyotaka Sakai,† and Teruo Okano*,‡

Department of Applied Chemistry, Waseda University, 3-4-1 Ohkubo, Shinjuku-ku, Tokyo 169-8555, Japan, and Institute of Advanced Biomedical Engineering and Science, Tokyo Women's Medical University, 8-1 Kawada-cho, Shinjuku-ku, Tokyo 162-8666, Japan

Received September 28, 2002; Revised Manuscript Received November 20, 2002

Acrylic acid (AAc) has been utilized to introduce reactive carboxyl groups to a temperature-responsive polymer, poly(*N*-isopropylacrylamide) (PIPAAm). However, AAc introduction shifts the copolymer phase transition temperatures higher and dampens the steep homopolymer phase transition with increasing AAc content. We previously synthesized 2-carboxyisopropylacrylamide (CIPAAm) having both a similar side chain structure to IPAAm and a functional carboxylate group in order to overcome these shortcomings. In the present study, these copolymers, grafted onto cell culture plastic, were assessed for cell adhesion control using their phase transition. AAc introduction to PIPAAm-grafted surfaces resulted in excessive surface hydration and hindered cell spreading in culture at 37 °C. In contrast, CIPAAm-containing copolymer-grafted surfaces exhibited relatively weak hydrophobicity similar to both homopolymer PIPAAm-grafted surfaces as well as commercial ungrafted tissue culture polystyrene dish surfaces. Cells adhered and spread well on these surfaces at 37 °C in culture. As observed previously on PIPAAm-grafted surfaces, cells were spontaneously detached from the copolymer-grafted surfaces by reducing culture temperature. Cell detachment was accelerated on the CIPAAm copolymer-grafted surfaces compared to pure IPAAm surfaces, suggesting that hydrophilic carboxyl group microenvironment in the monomer and polymer is important to accelerate grafted surface hydration below the lower critical solution temperature, detaching cells.

Introduction

Intelligent polymers that exhibit significant property changes in response to external stimuli such as temperature, pH, and ionic strength have been investigated for various applications such as controlled release of genes[1] and drugs[2,3] and enzymatic activity control.[4] Poly(*N*-isopropylacrylamide) (PIPAAm) is a temperature-responsive polymer, and we have utilized the unique polymer for separations,[5,6] controlled drug release,[7,8] gene delivery,[9] and cell−surface adhesion control.[10−13] Other monomers having reactive groups such as carboxylic acid have been introduced into PIPAAm as copolymers to immobilize various bioactive molecules.[14,15] However, introduction of polar moieties such as acrylic acid (AAc) to PIPAAm often affects the phase transition behavior.[3,16,17] Feil et al. reported the effect of comonomer hydrophilicity and ionization on the lower critical solution temperature (LCST) of *N*-isopropylacrylamide (IPAAm) copolymers.[18] They suggested that the excess hydration from AAc divides PIPAAm sequences into multiple short segments that reduce cooperative hydrophobic aggregation of PIPAAm chains at the phase transition. Continuity of pendant isopropylamide groups in the temperature-responsive polymer seems to contribute to the steep phase transition because the main mechanism of thermally induced phase separation involves cooperative thermal release of clustered water around aligned hydrophobic isopropyl groups. Therefore, we synthesized a novel functional monomer, 2-carboxyisopropylacrylamide (CIPAAm), whose structure consists of a vinyl group, isopropylamide group, and carboxyl group, which is distinct from AAc while analogous to IPAAm except for the carboxyl group.[19] P(IPAAm-*co*-CIPAAm) exhibits nearly the same LCSTs and temperature sensitivity as the IPAAm homopolymer.[19−21]

In the present study, cell adhesion and detachment behavior were examined in culture on the temperature-responsive surfaces grafted with PIPAAm, P(IPAAm-*co*-AAc), or P(IPAAm-*co*-CIPAAm). Because a surface phase transition associated with graft polymer hydration/dehydration has been shown critical for effective detachment of cultured cells, distinct difference in cell adhesion behavior were expected for AAc− vs CIPAAm−IPAAm copolymer surfaces. Acceleration of cell detachment is observed on CIPAAm surfaces over IPAAm homopolymer surfaces. Local influences of polar group water interaction are likely responsible for this behavior.

* To whom the correspondence should be addressed: e-mail, tokano@abmes.twmu.ac.jp; tel, +81-3-3353-8111, ext. 30233; fax, +81-3-3359-6046.

† Waseda University.

‡ Tokyo Women's Medical University.

10.1021/bm0256921 CCC: $25.00
Published on Web 01/03/2003

Experimental Section

Materials. *N*-Isopropylacrylamide (IPAAm) was kindly provided by Kojin Co. (Tokyo, Japan) and purified by recrystallization from *n*-hexane. 2-Carboxyisopropylacrylamide (CIPAAm) was synthesized as described previously.[19] Acrylic acid (AAc) was purchased from Wako Pure Chemicals Co. (Tokyo, Japan) and distilled under reduced pressure. Tissue culture polystyrene (TCPS) dishes (Falcon 3001) were purchased from Becton Dickinson Labware (Oxnard, CA). Trypsin−EDTA solution, streptomycin, and penicillin were bought from Gibco BRL (Grand Island, NY). Dulbecco's modified Eagle's medium (DMEM) was purchased from Iwaki (Chiba, Japan).

Preparation of Temperature-Responsive Culture Dishes. Temperature-responsive polymers, PIPAAm, P(IPAAm-*co*-CIPAAm), and P(IPAAm-*co*-AAc), were covalently grafted onto TCPS dishes as described previously.[10] Briefly, monomers were dissolved in 2-propanol at a concentration of 55% (wt/wt). For preparation of IPAAm copolymer-grafted surfaces, comonomers AAc or CIPAAm were added in ratios of 1, 3, and 5 mol % to total monomer concentration, respectively. These monomer solutions (30 μL) were spread uniformly over 35-mm TCPS dish surfaces, and electron beam is radiated to polymerize and covalent graft the dish surfaces using an area beam electron processing system (Curetron EBC-200-AA2, Nissin High Voltage Co. Ltd., Kyoto, Japan) at a radiation dose of 0.3 MGy (acceleration voltage of 150 kV under 1.0×10^{-4} Pa). Unreacted monomers and ungrafted polymers were removed by washing extensively with cold water, and the polymer-grafted TCPS dishes were dried in vacuo at room temperature.

Grafted polymer densities on TCPS dishes were determined by ATR-FTIR spectra (Jasco Valor-III, Tokyo). All samples were cut (1.0×3.0 cm) to be analyzed by attenuated total reflectance Fourier transform infrared (ATR-FTIR) spectroscopy. Since the base substrate was tissue culture grade polystyrene, the absorption at 1600 cm^{-1} arising from monosubstituted aromatic ring was compared to the strong absorption of amide in the region of 1650 cm^{-1}. The peak intensity ratio (I(1650)/I(1600)) was used to determine the graft density of polymers on the surface using the calibration curve given by analysis of PIPAAm cast on TCPS surfaces at known quantities.

Water Contact Angle Measurements. Temperature-responsive dishes were cut to 1.0×3.0 cm. Water contact angles were determined by a sessile drop method at either 20 or 37 °C with a FACE contact angle meter (the image processing type CA-X, Kyowa Interface Science, Saitama, Japan) using DMEM with serum as the probe solution. Three samples of each surface were measured five times and averaged.

Cell Culture. Bovine aortic endothelial cells (BAECs) were provided by the Health Science Research Resources Bank (JCRB 0099; Osaka, Japan). BAECs were cultured on TCPS dishes with DMEM supplemented with 10% fetal bovine serum (FBS), 100 units/mL penicillin, and 100 μg/mL streptomycin at 37 °C in humidified atmosphere with 5% CO_2. The BAECs were harvested from TCPS dishes with 0.25% trypsin−0.26 mM EDTA in Dulbecco's phosphate-buffered saline (PBS) and plated on polymer-grafted TCPS dishes. Cell morphology was monitored and photographed under a phase contrast microscope (ET300, Nikon, Tokyo).

Cell Spreading and Detachment. For cell spreading assay, BAECs were seeded at a density of 1.0×10^4 cells/cm^2 and cultured at 37 °C. The number of spread cells was counted on printed photographs taken at indicated time points ($n = 3$). For cell growth assay, BAECs were seeded at a density of 2.0×10^4 cells/cm^2 and cultured at 37 °C for 2 days. Cell number was counted on printed photographs and averaged ($n = 3$). Lifting of single BAECs from PIPAAm and P(IPAAm-*co*-CIPAAm)-grafted TCPS dishes was investigated by low-temperature treatment after incubation at 37 °C. For low-temperature treatment, spread cells were transferred to a CO_2 incubator equipped with a cooling unit fixed at 20 °C. Cell morphology was continuously observed and microphotographed under a phase contrast microscope. The spread cell number to the total cells was presented as a mean value ($n = 3$) and standard deviation. For confluently cultured cell sheets detachment assay, BAECs were plated onto each surface at a density of 2.0×10^5 cells/cm^2 and cultured at 37 °C. After 24 h of incubation, the unattached cells were removed by medium exchange. After 1 week of culture at 37 °C, each plate was transferred to the CO_2 incubator set at 20 °C. Each plate was continuously observed and microphotographed under a phase contrast microscope. The areas of remaining cell sheets relative to total areas were calculated and averaged as a mean value ($n = 5$) and standard deviation.

Results

Grafted polymer amounts on PIPAAm, P(IPAAm-*co*-AAc), and P(IPAAm-*co*-CIPAAm)-grafted surfaces from ATR-FTIR analysis were roughly equivalent: 1.9 ± 0.0, 1.8 ± 0.1, and 1.9 ± 0.1 μg/cm^2, respectively. The mole fraction of comonomer determined by titration of nonimmobilized copolymer was correlated with that in the feed. For example, in the case of 5 mol % of comonomer introduction in feed, P(IPAAm-*co*-CIPAAm) and P(IPAAm-*co*-AAc) indeed contained 4.8 and 4.6 mol % of carboxyate groups, respectively. LCSTs of P(IPAAm-*co*-AAc) shifted to higher temperatures with increasing AAc content.[19] Therefore, P(IPAAm-*co*-AAc)-grafted surfaces were markedly more hydrophilic by contact angle analysis at 37 °C with increasing carboxyl group content (Figure 1). These contact angles were obtained under physiological pH and ionic strength of DMEM. By contrast, P(IPAAm-*co*-CIPAAm) surfaces did not exhibit such LCST increase,[19,20] and P(IPAAm-*co*-CIPAAm)-grafted surfaces exhibited nearly the same wettability at 37 °C as that of PIPAAm-grafted surfaces as well as TCPS dishes (Figure 1).

As shown in Figure 2, cell attachment and spreading decrease on P(IPAAm-*co*-AAc)-grafted dishes with increasing AAc content, compared with cells on ungrafted TCPS and PIPAAm-grafted dishes. Cell attachment was not observed on the surface containing 5 mol % AAc. In contrast, P(IPAAm-*co*-CIPAAm)-grafted surfaces did not reduce cell

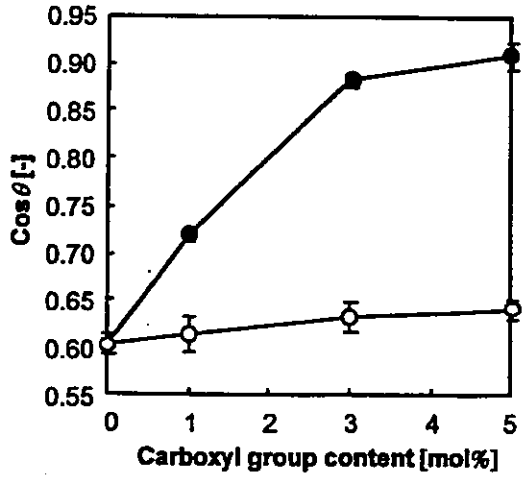

Figure 1. Surface wettability changes for P(IPAAm-*co*-CIPAAm) and P(IPAAm-*co*-AAc)-grafted TCPS dishes versus carboxyl monomer feed content at 37 °C measured by the sessile drop method. Dulbecco's modified Eagle's medium (DMEM) with serum was used as a probe solution. P(IPAAm-*co*-CIPAAm)-grafted surface (open circle) properties is independent of CIPAAm content while P(IPAAm-*co*-AAc)-grafted surface (closed circle) properties shift to more hydrophilic according to AAc content.

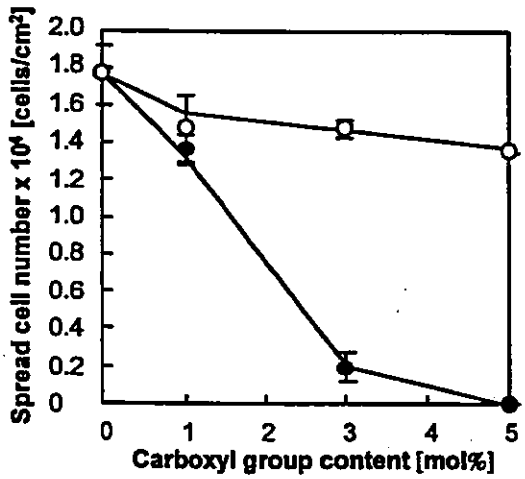

Figure 2. Spread BAECs number on P(IPAAm-*co*-CIPAAm) and P(IPAAm-*co*-AAc)-grafted TCPS dishes versus carboxyl group monomer feed content after 2 days of postseeding at 37 °C. Cells were seeded at a density of 2.0 × 10^4 cells/cm² onto these dishes. In contrast to spread cell numbers on P(IPAAm-*co*-CIPAAm)-grafted TCPS dishes (open circle), those on P(IPAAm-*co*-AAc)-grafted TCPS dishes (closed circle) are dramatically decreased because their surface LCSTs shift above 37 °C.

adhesion even at 5 mol % CIPAAm. Cell spreading was observed after 1 h of culture at 37 °C on both surfaces grafted with either PIPAAm or P(IPAAm-*co*-CIPAAm) and increased for both in a time-dependent manner (Figure 3). No difference in cell morphology was observed on these two surfaces. However, cell spreading on P(IPAAm-*co*-AAc)-grafted dishes was hardly observed even after 3 h of culture at 37 °C.

Culture temperature was reduced to 20 °C after 2 days at 37 °C. Within 15 min, 10% and 70% of single, spread, adherent cells came off from both PIPAAm-grafted and P(IPAAm-*co*-CIPAAm)-grafted dishes, respectively (Figure 4). For 90% cell detachment, 120 and 60 min were required

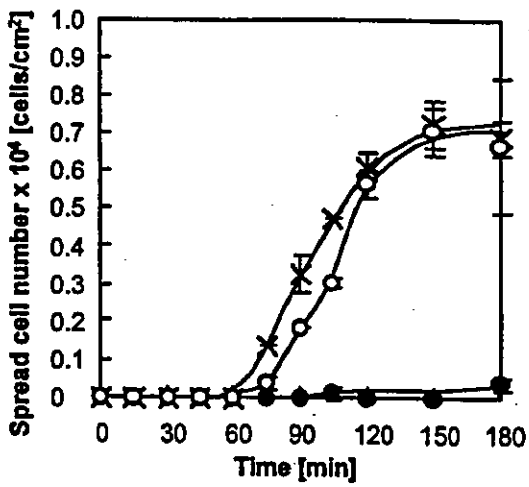

Figure 3. Spreading behavior of BAECs on PIPAAm, P(IPAAm-*co*-CIPAAm) (CIPAAm 1 mol % in feed), and P(IPAAm-*co*-AAc) (AAc 1 mol % in feed)-grafted TCPS dishes at 37 °C. Cells were seeded at a density of 1.0 × 10^4 cells/cm² onto these dishes. P(IPAAm-*co*-CIPAAm)-grafted TCPS dish (open circle) demonstrates increased spread cell number over time similar to the PIPAAm-grafted dish (cross) and cell morphologies exhibited on the two surfaces were very similar. In contrast, spread cells are scarcely observed on P(IPAAm-*co*-AAc)-grafted TCPS dishes (closed circle) 3 h postseeding.

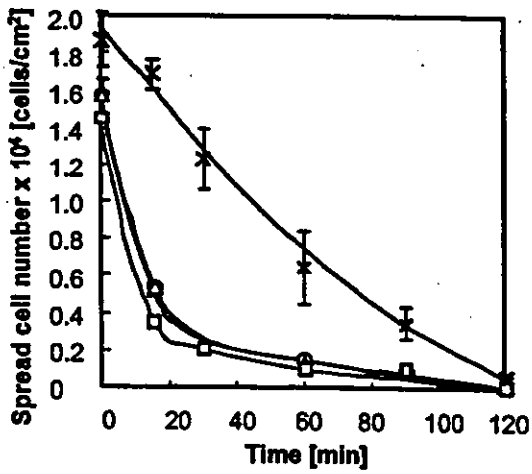

Figure 4. Cell lifting behaviors from grafted culture surfaces by reducing culture temperature below the LCST shown as the percentage of spread BAECs on PIPAAm (cross) and P(IPAAm-*co*-CIPAAm)-grafted TCPS dishes (1 mol % (open circle), 3 mol % (open triangle), 5 mol % (open square) CIPAAm in feed, respectively) as a function of incubation time at 20 °C. Cells were seeded at a density of 2.0 × 10^4 cells/cm² onto these dishes. Cells detach rapidly from P(IPAAm-*co*-CIPAAm)-grafted TCPS dishes compared to PIPAAm-grafted TCPS dishes.

for PIPAAm-grafted and P(IPAAm-*co*-CIPAAm)-grafted dishes, respectively. Cell shapes on P(IPAAm-*co*-CIPAAm)-grafted surfaces were rounded after 15 min due to loss of cell−substrate adhesion and cells began to lift off their surfaces.

In contrast, cell morphology changes on PIPAAm-grafted surfaces began to change after 60 min (Figure 5). The single cell detachment rate was more than three times higher on P(IPAAm-*co*-CIPAAm)-grafted dishes than on PIPAAm-grafted dishes (Figure 6). BAECs proliferated similarly on both these surfaces and reached confluency. By reduction

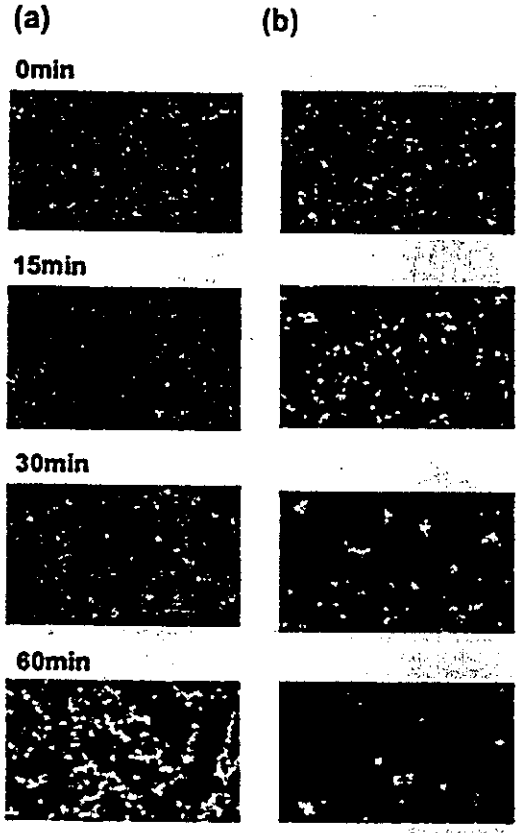

Figure 5. Phase-contrast photographs of BAEC detachment from PIPAAm (a) and P(IPAAm-*co*-CIPAAm) -grafted (CIPAAm 1 mol % in feed) (b) TCPS dishes. Cell morphologies on P(IPAAm-*co*-CIPAAm)-grafted surface become rounded and began to detach from these surfaces after 15 min.

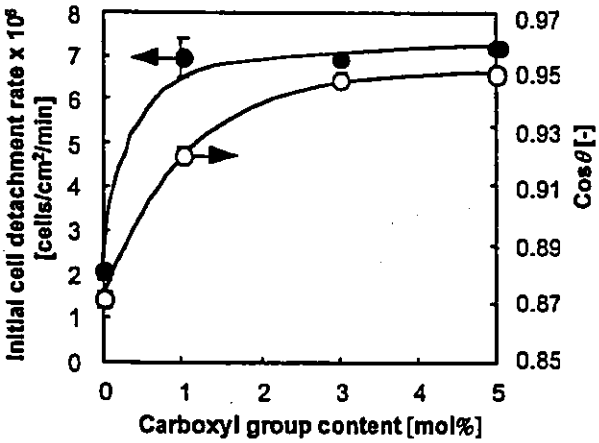

Figure 6. Surface wettability (cos θ) of P(IPAAm-*co*-CIPAAm)-grafted surfaces at 20 °C (below their LCSTs) (open circle) and initial cell detachment rates (closed circle) from these surfaces versus CIPAAm carboxyl group monomer feed content. Initial cell detachment rate is accelerated dramatically by introduction of CIPAAm while grafted surface wettability changes at 20 °C by the sessile drop method with a FACE contact angle meter are very small.

of the temperature to 20 °C, all confluent cells detached as a single contiguous cell sheet from the dish periphery. Cell sheet detachment occurred more quickly on P(IPAAm-*co*-CIPAAm)-grafted dishes than on PIPAAm-grafted dishes (Figure 7). The lag times were 40 and 15 min for PIPAAm-grafted and P(IPAAm-*co*-CIPAAm)-grafted dishes, respectively. BAECs did not reach confluency on P(IPAAm-*co*-AAc)-grafted surfaces even when AAc content was only 1 mol %.

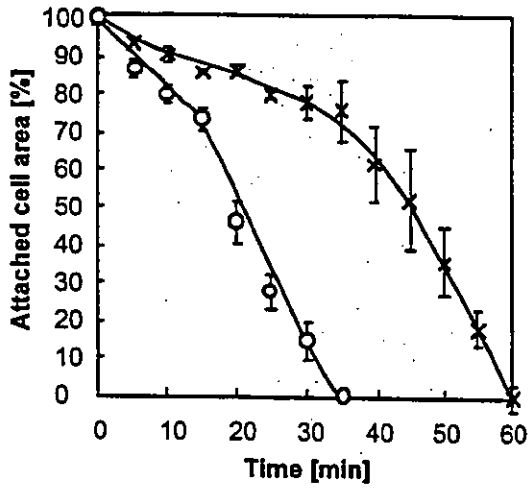

Figure 7. Cell sheet recovery from grafted surfaces by reducing culture temperature below the LCST, shown as the percentage of attached cell areas determined for cell sheets recovered from PIPAAm (cross) and P(IPAAm-*co*-CIPAAm)-grafted (CIPAAm 1 mol % in feed) (open circle) TCPS dishes as a function of incubation time at 20 °C. Cells are plated onto each surface at a density of 2.0×10^5 cells/cm^2. P(IPAAm-*co*-CIPAAm)-grafted surfaces demonstrated rapid cell sheet recovery.

Discussion

Incorporation of polar carboxyl groups into temperature-responsive PIPAAm increases polymer hydration and simultaneously increases their LCSTs by reducing cooperative hydrophobic aggregation forces above their LCSTs.[16,17] However, incorporation of the newly designed monomer, 2-carboxyisopropylacrylamide (CIPAAm), into PIPAAm overcomes this problem as its IPAAm-like structure apparently negligibly disturbs polymer LCST aggregation.[19-21] Hydrogels comprising both IPAAm and CIPAAm, P(IPAAm-*co*-CIPAAm), exhibit very large volume changes in response to temperature increases above their LCST, and the water content in these hydrogels is similar to that of IPAAm homopolymer hydrogel.[20,21] In contrast, CIPAAm copolymers swell more than IPAAm homopolymer gels below their LCST, as dissociated carboxyl groups promote gel swelling.[3,16-18] Previous studies show that carboxyl group acidity introduced into temperature-responsive PIPAAm increases with temperature reduction, due to the associated decreased dielectric constant within the polymer.[18,22] This can be explained by a reduced hydrophobicity (increasing hydration) of PIPAAm chains with temperature decrease. Several studies have shown that incorporation of hydrophobic comonomers into polyelectrolytes leads to a decrease in acidity. In the case of the PIPAAm hydrogel with carboxyl groups, polymer chain hydration and gel swelling below the LCST lead to increasing acidity, even if the swelling ratio above the LCST is unchanged with or without CIPAAm, because of the monomer's unique properties. In the present study, these intelligent polymer properties were investigated using their grafted surfaces in cell culture adhesion assays.

With ATR-FTIR, no differences are seen in polymer-grafted densities on TCPS surfaces between all three polymers grafted regardless of comonomer feed amounts. As seen in Figure 2, spread cell numbers on P(IPAAm-*co*-AAc)-grafted surfaces at 37 °C are decreased with increasing AAc copolymer content. Wettabilities of DMEM on P(IPAAm-*co*-AAc)-grafted surfaces also dramatically and consistently shift to hydrophilic (Figure 1) because surface gel phase transition temperatures are above 37 °C. As a result, BAECs are unable to adhere to them. In contrast, spread cell numbers on P(IPAAm-*co*-CIPAAm)-grafted surfaces at 37 °C are nearly identical to those on PIPAAm homopolymer-grafted surfaces. Contact angle data on these surfaces show that surface hydrophilicities increase negligibly with increasing CIPAAm content (Figure 1). IPAAm−CIPAAm chains apparently are able to maintain sufficient hydrophobic chain−chain interactions at 37 °C, and their LCSTs remain independent of carboxyl group content. Therefore BAECs attach, spread, and proliferate on P(IPAAm-*co*-CIPAAm)-grafted surfaces at 37 °C similar to that on PIPAAm-grafted surfaces despite introduction of carboxyl groups. As seen in Figure 3, P(IPAAm-*co*-CIPAAm)-grafted surfaces also demonstrate increased spread cell number over time very similar to PIPAAm-grafted dishes, and cell morphologies exhibited on the two surfaces are very similar. These results indicate that surface wettability correlates well to spread cell number on these surfaces.

Cell detachment assays from polymer-grafted surfaces by reducing culture medium temperature show that introduction of CIPAAm into PIPAAm chains significantly accelerates cell detachment rates despite similar cell attachment rates to PIPAAm-grafted surfaces (Figures 4−6). As described above, P(IPAAm-*co*-CIPAAm) possesses similar hydrophobicity as PIPAAm at 37 °C (above the LCST). Yet, the copolymer surfaces become more hydrophilic than PIPAAm homopolymer at 20 °C (below LCST) because amounts of charged carboxylate groups on the copolymers increase with decreasing temperature, as described above. Previous studies point out that hydration of ionized carboxylate groups is much larger than that of protonated carboxyl groups.[23,24] Acceleration of polymer hydration grafted on these surfaces promotes rapid surface swelling and subsequent cell lifting from them. We had already developed rapid cell recovery systems using two methodologies. First, PIPAAm was grafted onto porous membranes instead of TCPS to accelerate the hydration of hydrophobized PIPAAm segments interacting with adherent cell sheets.[25] The rate-limiting step to cell sheet recovery is the underlying polymer hydration beneath the cell sheet, and then water could be only supplied for polymer hydration from the cell sheet periphery. In contrast, with porous membrane, the water can access the grafted polymer not only from the periphery but also from beneath, resulting in rapid hydration of grafted PIPAAm and cell sheet detachment. Second, poly(ethylene glycol) (PEG) incorporation into these PIPAAm-grafted porous substrates as hydrophilic sites achieved much more rapid cell sheet recovery.[26] The grafted PEG chains enable promotion of the water molecule diffusion into the grafted PIPAAm layer in addition to the high water permeation effect based on the porous structure. In the PEG introduction technique, however, there is the limitation that PEG introduction also promotes the polymer hydration even above the LCST, resulting in restraint of cell adhesion. Introduction of more than 0.5 wt % of PEG into PIPAAm chains leads to dramatic cell adhesion decrease.

Surface wettability (cos θ) of PIPAAm-grafted surfaces changes from 0.60 (see Figure 1) to 0.87, indicating that surface properties become increasingly hydrophilic to a point where BAECs cannot adhere. The value of cos θ for P(IPAAm-*co*-CIPAAm)-grafted surfaces at 20 °C increases with increasing CIPAAm content. As can be seen in Figure 7, initial cell lifting rates from PIPAAm-grafted surfaces with decreasing temperature increase more than three times by introducing only a few percent of CIPAAm. The surface at 20 °C, however, became only slightly more hydrophilic with increasing grafted carboxyl group content (cos θ value changes from 0.87 to 0.95 by incorporation of 3 mol % carboxyl groups) while initial cell detachment rates are accelerated dramatically. Data shown here contrasting surface wettability and cell attachment/detachment for equally charged, compositionally equivalent carboxylate-containing IPAAm copolymers containing either CIPAAm or AAc seem to suggest nonequivalence of carboxylate polarity or structural presentation between CIPAAm and AAc. Phase transitions, swelling degrees, surface polarities, and cell−surface behavior are all substantially different for these IPAAm copolymer families. Acrylic acid has its carboxylate group directly adjacent to the polymer backbone, while CIPAAm extends its carboxylate group well away from the backbone. This change is in local microenvironment in different local dielectric constants, charges in carboxylate pK_a, and structural differences associated with various possible modes of hydrogen bonding between carboxylate (dimerization) and with acrylamide (−NHC=O) chemistries. While the exact nature of these differences in chemistry and their impact can only be speculative, experimental evidence consistently supports drastically different carboxylate microenvironments between these CIPAAm and AAc chemistries in their grafted networks on surfaces. Similar cooperative swelling/deswelling and wettability phenomena between IPAAm homopolymers and CIPAAm−IPAAm copolymers support an interpretation where an abrupt phase transition and therefore critical dehydration/hydration mechanisms are maintained in both systems. The difference nature of the IPAAm−AAc phase transition[3,18,19] supports an explanation of noncritical, noncooperative transitions with higher order mechanisms. These differences are readily distinguished by the cell phenomena where surface hydration for IPAAm and CIPAAm−IPAAm indicates a critical transition. These results indicate that slight hydrophobic/hydrophilic changes on these surfaces, difficult to determine by physicochemical measurements, can be ascertained by using culture cells as sensitive probes. The P(IPAAm-*co*-CIPAAm)-grafted surfaces facilitates rapid cell recovery without restraint of cell attachment and has a potential that various bioactive peptides and proteins such as synthetic cell adhesive peptides and growth factors can be immobilized via carboxyl groups to control cell proliferation and differentiation by temperature

changes. These functionalizations endow temperature-responsive dishes with more utility for cell culture and tissue engineering including serum-free culture.

Acknowledgment. We are grateful to Professor D. W. Grainger (Colorado State University, USA) for continued discussion. The present study was supported in part by Japan Ministry for Culture, Sports, Education, Science and Technology, Core Research for Evolutional Science and Technology (CREST).

References and Notes

(1) Kyriakides, T. R.; Cheung, C. Y.; Murthy, N.; Bornstein, P.; Stayton, P. S.; Hoffman, A. S. *J. Controlled Release* **2002**, *78*, 295−303.
(2) Ramkissoon-Ganorkar, C.; Liu, F.; Baudys, M.; Kim, S. W. *J. Controlled Release* **1999**, *59*, 287−298.
(3) Yu, H.; Grainger, D. W. *J. Appl. Polym. Sci.* **1993**, *49*, 1553−1563.
(4) Ding, Z.; Fong, R. B.; Long, C. J.; Stayton, P. S.; Hoffman, A. S. *Nature* **2001**, *411*, 59−62.
(5) Yakushiji, T.; Sakai, K.; Kikuchi, A.; Aoyagi, T.; Sakurai, Y.; Okano, T. *Anal. Chem.* **1999**, *71*, 1125−1130.
(6) Kikuchi, A.; Okano, T. *Prog. Polym. Sci.* **2002**, *27*, 1165−1193.
(7) Okano, T., Ed. *Biorelated Polymer and Gels: Controlled of Release and Applications in Biomedical Engineering*; Academic Press: Chestnut Hill, MA, 1998.
(8) Okano, T.; Yui, N.; Yokoyama, M.; Yoshida, R. *Advances in Polymeric Systems for Drug Delivery*; Gordon & Breach: Yverdon, Switzerland, 1994.
(9) Kurisawa, M.; Yokoyama, M.; Okano, T. *J. Controlled Release* **2000**, *69*, 127−137.
(10) Yamada, N.; Okano, T.; Sakai, H.; Karikusa, F.; Sawasaki, Y.; Sakurai, Y. *Macromol. Chem. Rapid Commun.* **1990**, *11*, 571−576.
(11) Okano, T.; Yamada, N.; Okuhara, M.; Sakai, H.; Sakurai, Y. *Biomaterials* **1995**, *16*, 297−303.
(12) Yamato, M.; Konno, C.; Kushida, A.; Hirose, M.; Utsumi, M.; Kikuchi, A.; Okano, T. *Biomaterials* **2000**, *21*, 981−986.
(13) Kushida, A.; Yamato, M.; Konno, C.; Kikuchi, A.; Sakurai, Y.; Okano, T. *J. Biomed. Mater. Res.* **2000**, *51*, 216−223.
(14) Houseman, B. T.; Mrksich, M. *Biomaterials* **2001**, *22*, 943−955.
(15) Stile, R. A.; Healy, K. E. *Biomacromolecules* **2001**, *2*, 185−194.
(16) Chen, G.; Hoffman, A. S. *Nature* **1995**, *373*, 49−52.
(17) Kaneko, Y.; Nakamura, S.; Sakai, K.; Aoyagi, T.; Kikuchi, A.; Sakurai, Y.; Okano, T. *Macromolecules* **1998**, *31*, 6099−6105.
(18) Feil, H.; Bae, Y. H.; Feijen, J.; Kim, S. W. *Macromolecules* **1993**, *26*, 2496−2500.
(19) Aoyagi, T.; Ebara, M.; Sakai, K.; Sakurai, Y.; Okano, T. *J. Biomater. Sci., Polym. Ed.* **2000**, *1*, 101−110.
(20) Ebara, M.; Aoyagi, T.; Sakai, K.; Okano, T. *Macromolecules* **2000**, *33*, 8312−8316.
(21) Ebara, M.; Aoyagi, T.; Sakai, K.; Okano, T. *J. Polym. Sci., Part A: Polym. Chem.* **2001**, *39*, 335−342.
(22) Kobayashi, J.; Kikuchi, A.; Sakai, K.; Okano, T. *Anal. Chem.* **2001**, *73*, 2027−2033.
(23) Jones, M. S. *Eur. Plym. J.* **1999**, *35*, 795−801.
(24) Yoo, M. K.; Sung, Y. K.; Lee, Y. M.; Cho, C. S. *Polymer* **2000**, *41*, 5713−5719.
(25) Kwon, O. H.; Kikuchi, A.; Yamato, M.; Sakurai, Y.; Okano, T. *J. Biomed. Mater. Res.* **2000**, *50*, 82−89.
(26) Kwon, O. H.; Kikuchi, A.; Yamato, M.; Okano, T. *Biomaterials*, in press.

BM025692T

TISSUE ENGINEERING
Volume 9, Number 5, 2003

Transplantable Urothelial Cell Sheets Harvested Noninvasively from Temperature-Responsive Culture Surfaces by Reducing Temperature

YOSHIYUKI SHIROYANAGI, M.D.,[1,2] MASAYUKI YAMATO, Ph.D.,[1]
YUICHIRO YAMAZAKI, M.D.,[2] HIROSHI TOMA, M.D.,[2] and TERUO OKANO, Ph.D.[1]

ABSTRACT

Augmentation cystoplasty using gastrointestinal flaps may induce severe complications such as lithiasis, urinary tract infection, and electrolyte imbalance. The use of viable, contiguous urothelial cell sheets cultured *in vitro* should enable us to avoid these complications. Transplantable urothelial cell sheets were obtained by utilizing a temperature-responsive cell culture method, and then examined by immunostaining and electron microscopy. Canine urothelium was produced on the surfaces of temperature-responsive culture dishes covalently bonded with the thermally sensitive polymer, poly(*N*-isopropylacrylamide). Stratified urothelial cell sheets were cultured and then harvested intact without enzymatic treatment from these dishes by reducing the temperature. Histological structure and cell-to-cell junctions were compared between these urothelial cell sheets and those harvested with dispase. All urothelial cell sheets were harvested from the bonded surfaces by reducing the culture temperature without the need for dispase. Electron microscopy revealed well-developed microridge, microvilli, and cell junction complexes. Conversely, these same cell features were destroyed by dispase treatment. Immunoblotting revealed that dispase fragmented occludin, whereas it remained unchanged in the intact urothelial cell sheets. Novel urothelial cell sheets obtained by culture on temperature-responsive culture surfaces were successfully harvested much less destructively than with dispase. This technology should prove useful in urinary tract tissue engineering in the near future.

INTRODUCTION

MODERN TISSUE-ENGINEERING TECHNIQUES would potentially allow for various augmentation methods of the urinary bladder[1–3] to avoid the complications of augmentation cystoplasty and reconstruction of the urinary bladder using gastrointestinal flaps. The majority of late complications from these conventional procedures, including stone formation, urinary tract infection, electrolyte imbalance, mucous production, and carcinoma, are related to the intestinal mucosa. Therefore, techniques of autoaugmentation cystoplasty have focused on using demucosalized seromuscular intestinal flaps. Although some investigators have reported good results after seromuscular entrocystoplasty,[4,5] others have obtained poor results.[6,7] Because contact with urine frequently induces severe fibrosis and contraction in the exposed surface of the seromuscular flaps,[7] alternative approaches have been developed to avoid urinary contact with these flaps, including use of urothelial lined intestinal flaps.[8] However, the size of the native urothelium is a limiting factor for bladder capacity. Aktug *et al.*[9] reported that prefabricated

[1]Institute of Advanced Biomedical Engineering and Science and [2]Department of Urology, Tokyo Women's Medical University, Tokyo, Japan.

seromuscular intestinal flaps resulted in good performance when the surface of the seromuscular flap was partially grafted with urothelium before use. Simultaneously, they noted the disadvantages of prefabricated enterocystoplasty, especially the necessity for a two-stage operation and opening of the bladder to obtain the urothelium. Clearly, this therapeutic intervention would benefit from alternative sources of tissues suitable for flap construction.

Previous work in our laboratory has shown that various intact cell sheets from diverse primary sources can be harvested without enzymatic methods by using temperature-responsive culture dishes.[10,11] A temperature-responsive polymer, poly(*N*-isopropylacrylamide) (PIPAAm),[12] is bonded onto commercially available culture dish surfaces by electron beam irradiation. This surface is slightly hydrophobic in culture at 37°C, and hydrates spontaneously below the polymer's lower critical solution temperature (LCST) of about 32°C to make its surface hydrophilic. When the culture temperature is reduced below the LCST, the cells spontaneously detach from the surface because of rapid hydration of the bonded PIPAAm chains. Intact, with cell-to-cell junctions, the cells often are recovered as a single, contiguous sheet.[10,11]

Cells harvested from temperature-responsive surfaces by reducing the temperature maintain highly differentiated functions compared with similar cells recovered by trypsinization. Such low-temperature treatment appears, then, to be less destructive to cells. Using this technology, we have now investigated the feasibility of replacing gastrointestinal mucosa with cultured urothelial cell sheets. In the present report, we describe the harvest of intact urothelial cell sheets without dispase, and the further examination of the harvested cell sheets.

MATERIALS AND METHODS

Isolation of urothelial cells from canine bladders

Urinary bladders were obtained from beagle dogs (10–12 kg). All experimental protocols were approved by the animal welfare committee of Tokyo Women's Medical University (Approval No. 02-55, 2002). Each dog was anesthetized with sodium pentobarbital (50 mg/kg) and killed by exsanguination. A laparotomy was made via a midline incision and a cystectomy was performed. The protocol described by Fujiyama *et al.*[13] with certain modifications was used to isolate bladder epithelium. The bladder was cut into halves, and the smooth muscle layer was removed with scissors. The epithelial layer attached to the lamina propria was cut into rectangles and treated with dispase solution (1000 U/mL; Godoshusei, Tokyo, Japan) overnight at 4°C. After the enzymatic treatment, the epithelial layer was peeled from the stromal layer with forceps under a microscope. The epithelial layer was digested in 0.1% trypsin–ethylenediaminetetraacetic acid (EDTA) solution (GIBCO-BRL Life Technologies, Grand Island, NY) for 5 min at 37°C. The single-cell suspension was filtered through 100-μm nylon cloth and centrifuged at 800 rpm for 5 min. The supernatant was aspirated carefully and the cells were washed an additional two times.

Preparation of square-designed temperature-responsive cell culture surfaces

Specific procedures for the preparation of pattern-designed PIPAAm-bonded cell culture dishes are described elsewhere.[14] Briefly, *N*-isopropylacrylamide (IPAAm) monomer (kindly provided by Kohjin, Tokyo, Japan) in 2-propanol solution was spread onto tissue culture polystyrene dishes. The dishes were then subjected to irradiation with a 0.25-MGy electron beam, using an area beam electron processing system (Nisshin High Voltage, Kyoto, Japan). IPAAm was simultaneously polymerized and bonded onto the dish surfaces. The PIPAAm-bonded dishes were rinsed with cold distilled water to remove nonbonded IPAAm. For the second step, the PIPAAm-bonded surfaces were masked with glass coverslips (24 × 24 mm), and irradiated after acrylamide (AAm) (Wako Pure Chemicals, Tokyo, Japan) was spread across the surface. The dish surfaces were then washed after this bonding reaction. Glass-masked square areas of coverslip dimensions remained PIPAAm bonded (temperature responsive) while the surrounding area was poly-AAm bonded (noncell adhesive). The bonded amount of PIPAAm used in the present study was estimated as 2 μg/cm^2.

Urothelial cell culture

Dissociated urothelial cells (~1–2 × 10^5/cm^2) were seeded in the designed PIPAAm dish and cultured according to the method of Rheinwald and Green[15] with a feeder layer of mitomycin C-treated NIH 3T3 cells to which was added Ham's F12 medium–DMEM in a 1:3 ratio supplemented with 5% fetal bovine serum, insulin (5.0 μg/mL), transferrin (5.0 μg/mL), triiodothyronine (2 nM), cholera toxin (1 nM), hydrocortisone (0.4 μg/mL), recombinant human epidermal growth factor (10 ng/mL; GIBCO-BRL Life Technologies), recombinant fibroblast growth factor 7 (FGF-7, 100 ng/mL; R&D Systems, Minneapolis, MN), penicillin, and streptomycin.

Recovery of urothelial cell sheets from the temperature-responsive culture surfaces

The urothelial cells were cultured for 3 weeks. All confluent urothelial cells were recovered from the PIPAAm-bonded dishes by three different methods: low-temperature treatment, dispase treatment, and physical scraping

with a rubber blade. In the low-temperature treatment, the temperature-responsive culture dishes were incubated at 20°C for 30 min and the urothelial cell sheets detached spontaneously from the dishes. In the dispase treatment, the urothelial cell sheets were removed after incubation with dispase II (2.5%; Roche Diagnostics, Mannheim, Germany) at 37°C for 30 min. The harvested urothelial sheets were washed three times with Dulbecco's phosphate-buffered saline (PBS) containing a protease inhibitor cocktail (Wako, Osaka, Japan) and phenylmethylsulfonyl fluoride (1 mM; Sigma, St. Louis, MO), and lysed in lysis buffer (20 mM Tris-buffered saline [TBS] containing 0.1% sodium dodecyl sulfate, 8 M urea, and the protease inhibitors). In the physical scraping method, the cell layers were removed from the dish surfaces with a rubber blade with lysis buffer.

Immunoblotting

Whole cell lysates were electrophoresed on a 7.5% polyacrylamide gel. Resolved proteins on a polyacrylamide gel were electrophoretically transferred to a poly(vinylidene difluoride) transfer membrane (80 V for 3 h). The membrane was incubated at 4°C for 24 h in a blocking solution, and probed with rabbit anti-occludin polyclonal antibody (diluted 1:1000; Zymed Laboratories, South San Francisco, CA) at room temperature for 1 h. After extensive washing, the membrane was further incubated with a 1:10,000 dilution of horseradish peroxidase-conjugated sheep anti-rabbit immunoglobulin antibody at room temperature for 1 h, and the bands of occludin were detected by chemiluminescence of the product of a peroxidase reaction, using the ECL system (Amersham, Buckinghamshire, UK).

Histology and immunohistochemistry

Urothelial cell sheets were dehydrated through a graded series of ethanol to xylol, embedded in paraffin, and cut at 10 μm for hematoxylin and eosin staining. For immunohistochemistry, paraffin tissue sections of the grafts were mounted on glass slides, deparaffinized in xylol and dehydrated. Thereafter, the sections were subjected to enzymatic pretreatment with proteinase K (DakoCytomation, Glostrup, Denmark). The sections were then stained with diluted rabbit antiserum to total bovine uroplakins (kindly provided by T.T. Sun, New York University, New York, NY), using an LASB kit (DakoCytomation), and counterstained with hematoxylin. Frozen tissue blocks of the recovered urothelial cell sheets were cut with a microtome into 10-μm sections, and mounted on glass slides. The sections and the urothelial cell sheets were fixed at room temperature with 4% paraformaldehyde in PBS for 20 min. They were then washed with PBS, permeabilized with 0.5% Triton X-100 in PBS for 5 min, washed three times with PBS, and blocked with 0.1% bovine serum albumin fraction V (BSA) in PBS for 120 min. The primary antibodies used were mouse monoclonal anti-human cytokeratin (AE1/AE3; DakoCytomation), rabbit polyclonal anti-bovine fibronectin (Biogenesis, Poole, UK) and rabbit polyclonal anti-occludin (Zymed Laboratories). Sections and sheets were incubated with the primary antibodies for 24 h, rinsed with PBS three times, and incubated for 2 h with the secondary FITC-conjugated goat anti-mouse antibody or with FITC-conjugated goat anti-rabbit antibody (ICN Immunobiologicals, Costa Mesa, CA), depending on the primary antibody. For nuclear staining, the sections were costained with a DNA-binding dye (Hoechst 33258, Molecular Probes, Eugene, OR).

Electron microscopy

Urothelial cell sheets harvested from PIPAAm dishes by either dispase treatment or low-temperature treatment were cut into small pieces of approximately 1 mm^3, fixed in 2.5% glutaraldehyde for 2 h, washed with cacodylate buffer, postfixed in 1.0% osmium tetroxide, and dehydrated through graded alcohols. The samples were embedded in Quetal 812 (Nisshin, Tokyo, Japan) and ultrathin sections (90 nm) were cut on an ultramicrotome with a diamond knife, and then stained with uranyl acetate and lead citrate. The sections were examined at 80 kV under a transmission electron microscope. Other samples were cut into small pieces, fixed in 2.5% glutaraldehyde for 1 h, postfixed in 1.5% osmium tetroxide, dehydrated through graded alcohols, dried by the *t*-butyl alcohol method, and osmium sputtered for 15 s. These samples were examined with a scanning electron microscope.

RESULTS

Canine urothelial cells were cultured according to the 3T3 feeder layer method[15] on the square-designed surfaces bonded with a temperature-responsive polymer, PIPAAm. The urothelial cells adhered, spread, and proliferated to confluency, and partial stratification was induced on the bonded dishes over 3 weeks of culture at 37°C (Fig. 1A). These stratified urothelial cells were subjected to a novel harvesting method without the use of dispase. The cells were simply incubated at 20°C, and the urothelial cell sheets peeled spontaneously from the PIPAAm-bonded dishes within 30 min. The urothelial cell sheets were carefully harvested from the dishes with fine forceps. By this method, all of the urothelial cells were recovered and no cell remnants were observed on the dish surfaces. After detachment, the urothelial cell sheets contracted slightly (Fig. 1B), and conventional histology showed the presence of one to four cell layers (Fig. 1C).

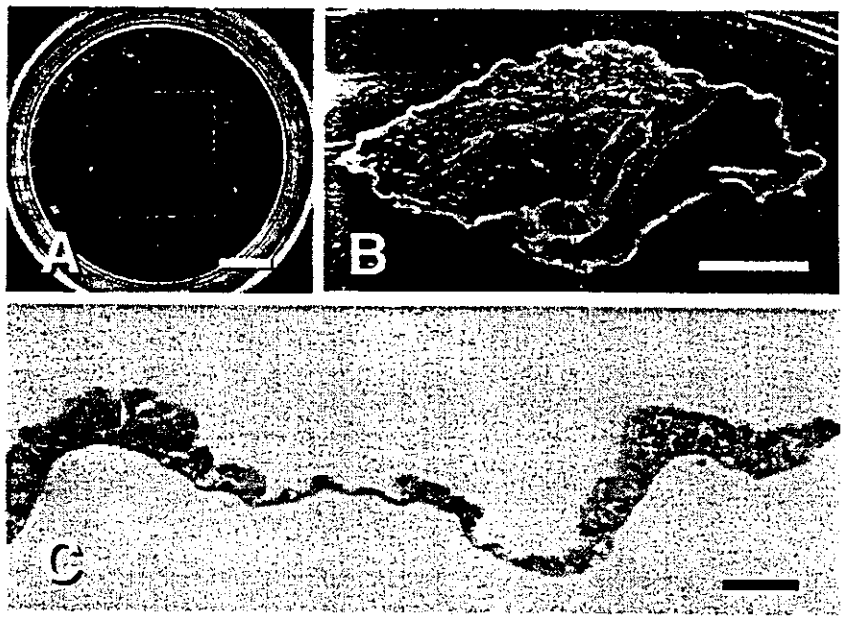

FIG. 1. Transplantable urothelial cell sheets. Primary urothelial cells were cultured on square-pattern-designed temperature-responsive culture dishes at 37°C for 3 weeks (A). Macroscopic view of an urothelial cell sheet harvested by reducing temperature (B). H&E staining of the histological sections revealed the monolayer and multilayer of urothelial cell sheet (C). Scale bars: (A and B) 1 cm; (C) 100 μm.

Scanning electron microscopy revealed a cobblestone-like appearance of the urothelial cells, which had four to seven sides (Fig. 2A). Microplicae and microvilli, typical of differentiated apical urothelial cells, were present in urothelial cell sheets harvested by the low-temperature treatment (Fig. 2B). Conversely, these features were fewer, or each microplicum did not appear to form indentations in the urothelial cell sheets recovered by dispase treatment (Fig. 2C and D). Transmission electron microscopy demonstrated morphological stratification and a polarized structure of cells in the urothelial cell sheets harvested by the low-temperature treatment (Fig. 2E and F). Numerous vesicles occupied the apical cytoplasm of superficial cells in the urothelial cell sheets (Fig. 2F). Junction complexes were also observed between adjacent lumenal urothelial cells (Fig. 2G).

The urothelial cell sheets were positively stained with anti-cytokeratin antibody (AE1/AE3) (Fig. 3A) and anti-uroplakin antibody, which is a specific marker of differentiated urothelium (Fig. 3B). Deposited fibronectin was observed at the bottom of urothelial cell sheets harvested by the low-temperature treatment (Fig. 3C and D). Occludin, one of the major constituents of tight junctions, was observed by its "honeycomb-like" morphology in the urothelial sheets (Fig. 3E).

Recovered urothelial cells were subjected to immunoblotting with anti-occludin antibody (Fig. 4). Occludin (molecular mass, 62–82 kDa; multiple band) was detected with intact molecular size in cell lysates obtained by low-temperature treatment or physical scraping. In contrast, dispase treatment disrupted occludin into fractions of smaller molecular size.

DISCUSSION

To develop a cell culture model of uroepithelium, several systems have been described and stratified urothelial constructs have been induced *in vitro*, resembling native urothelium.[13,16,17] We obtained stratified urothelial cell sheets according to the 3T3 feeder layer method widely used for the preparation of multilayered epithelial cells,[15] with slightly modified culture medium containing FGF-7. Tash *et al.*[17] reported that FGF-7 was essential for normal bladder urothelial stratification, specifically for the formation of the intermediate cell layers. Electron microscopy revealed that harvested stratified urothelial cell sheets consisted of differentiated cell layers comprising superficial, intermediate, and basal cell types (Fig. 2). The 3T3 feeder layer method, originally described by Rheinwald and Green,[15] is generally accepted for making clinically available cultured epidermal graft. Although the fibroblasts are growth-arrested with mitomycin C before their use as feeder layers, 3T3 fibroblasts are still metabolically active, secreting various factors thought to contribute to the adhesion and prolif-

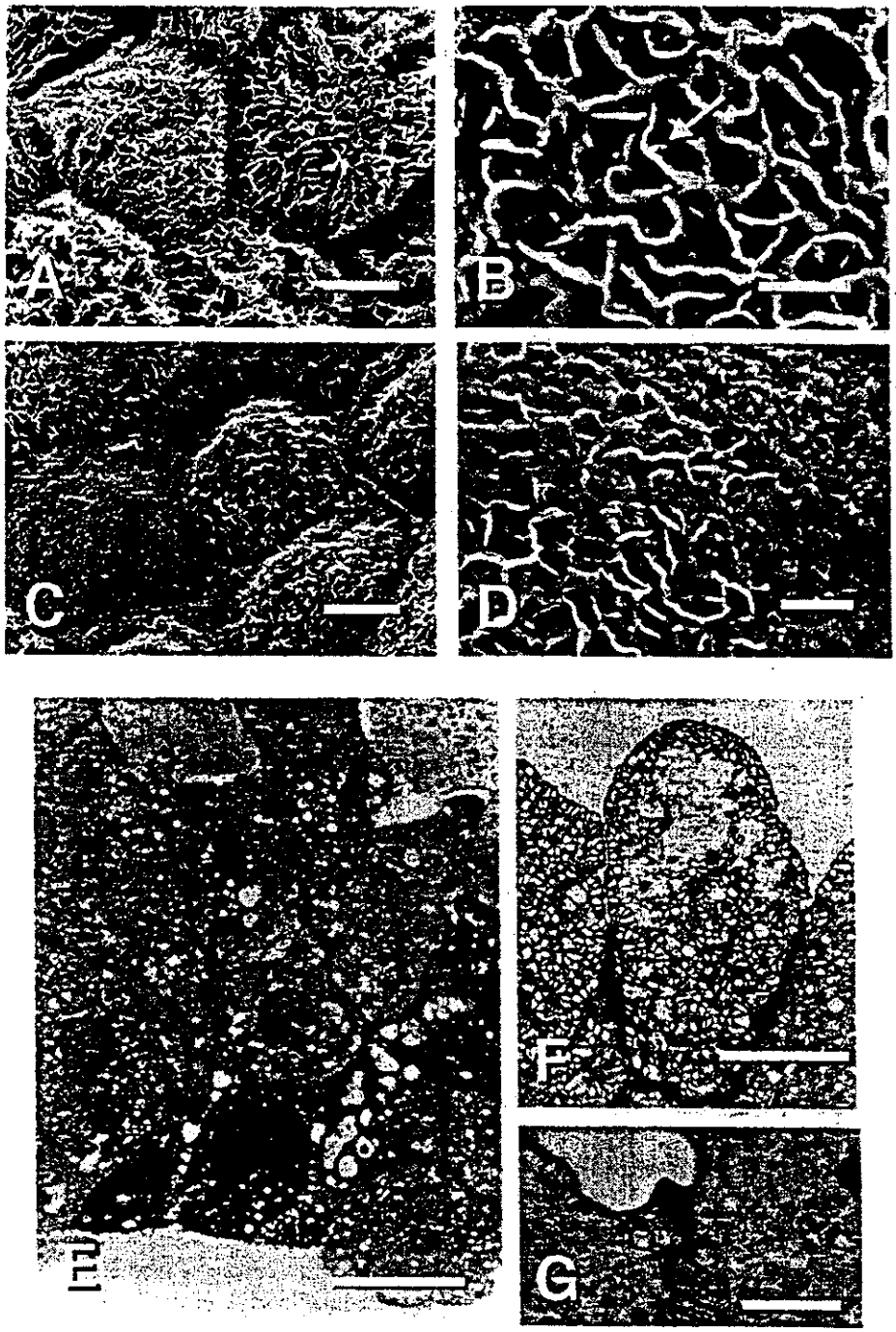

FIG. 2. Electron microscopy of harvested urothelial cell sheets. Scanning electron microscopy revealed that the apical surfaces of multilayered urothelial cell sheets harvested by low temperature treatment showed characteristics of differentiated urothelial superficial cells including microvilli (arrow) on fine microridges (**A** and **B**). However, similar cell sheets harvested with dispase lost such microstructures (**C** and **D**). Completely and partially destroyed microvilli were observed on the same cell surface (**D**). Transmission electron microscopy of multilayered urothelial cell sheets, which were harvested by low temperature treatment (**E–G**). In the intermediate cells in the urothelial cell sheets, extensive interdigitation was observed (**E**). The nuclei of the intermediate cells contain rather less chromatin and smaller nucleoli than the basal cells as shown *in vivo* (**E**). Note the differentiated characteristics of superficial cells such as numerous vesicles in cytoplasm (**F**) and tight junctions (**G**). Scale bars: (**A** and **C**) 5 μm; (**B**, **D**, and **G**) 1 μm; (**E** and **F**) 10 μm.

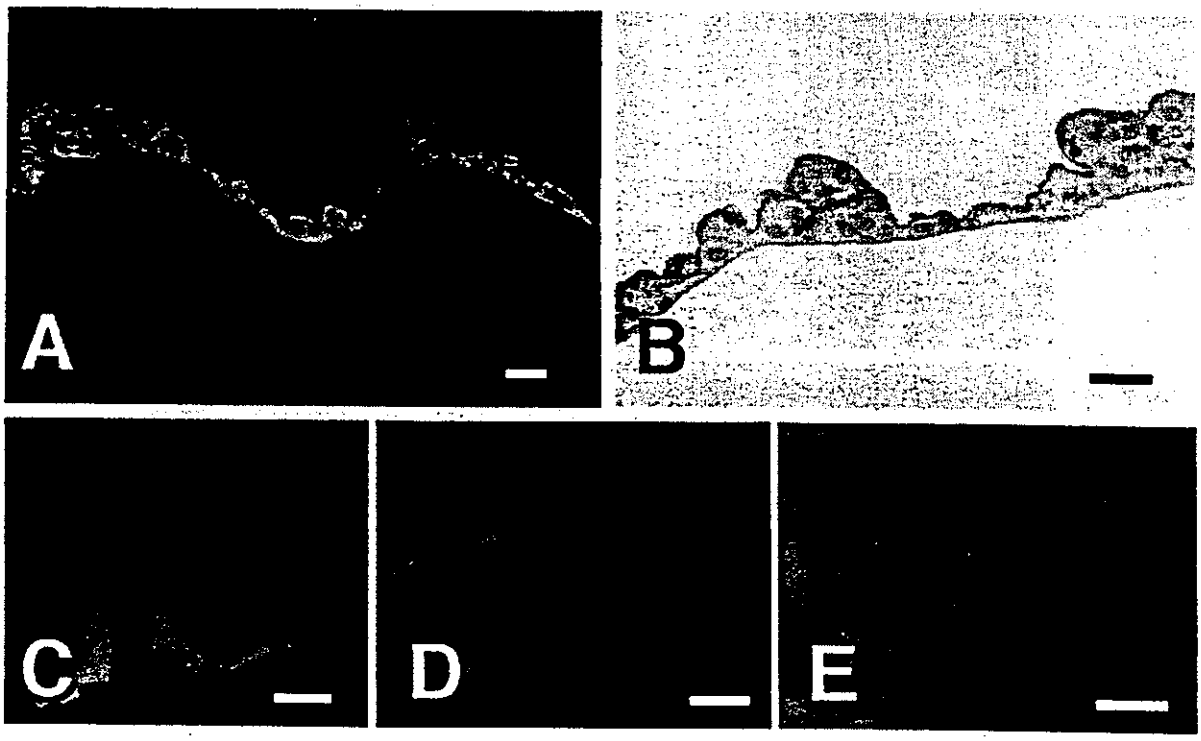

FIG. 3. Immunohistochemistry of urothelial cell sheets harvested by low-temperature treatment. Anti-pancytokeratin antibodies (AE1/AE3) positively stained the entire cell layer of harvested urothelial cell sheets (A). Anti-asymmetric unit membrane antibody, uroplakin, positively stained the apical cell surfaces (B). Anti-fibronectin antibody specifically stained the bottom of harvested urothelial cell sheets (C) that were costained with the DNA-binding dye shown in (D). Anti-occludin antibody stained the entire cell periphery between adjacent cells of the cell sheet observed in a bird's-eye view (E). Scale bars: (A and B) 100 μm; (C and D) 20 μm; (E) 10 μm.

eration of epidermal stem and differentiated cells. In the present study, we also observed that urothelial cells cultured with a 3T3 feeder layer were cuboidal in cell morphology and less fragile (data not shown).

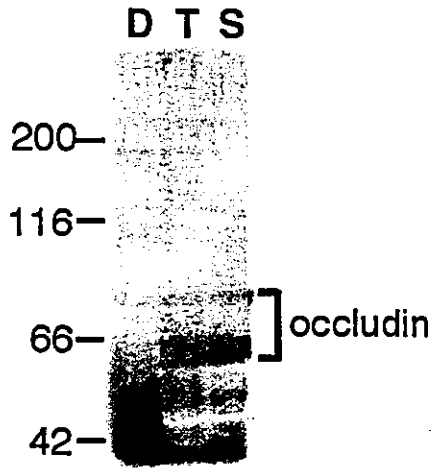

FIG. 4. Immunoblotting of urothelial cell sheets recovered from temperature-responsive dishes with anti-occludin antibody. Lane D, dispase II treatment; lane T, low-temperature treatment. lane S, physical scraping with rubber blades.

From our previous studies with other cell types, we understand the detachment mechanisms of the cells and cell sheets from temperature-responsive culture dishes to be as follows. In temperature-responsive cell detachment from PIPAAm-bonded dishes, both "passive" and "active" mechanisms are required. The passive mechanism is related to the surface change from slightly hydrophobic to highly hydrophilic obtained by reducing the temperature below the LSCT. Cells generally adhere to slightly hydrophobic surfaces. Cell adhesion to slightly hydrophobic surfaces is mediated by the adsorption of extracellular matrix proteins onto the surfaces. These cell-adhesive proteins and/or receptors are degraded by dispase treatment, and the attached cells become detached. Conversely, temperature-responsive PIPAAm-bonded surfaces rapidly become highly hydrophilic below the LSCT. Hydrophilic surfaces release the adsorbed proteins. Second, the active mechanism of cell detachment is related to ATP-dependent cell metabolism. Active energy-dependent processes mediated by intracellular signal transduction, including tyrosine phosphorylation and cytoskeletal reorganization, lead to morphological change of the cell from spreading to round after the change in the surface property.[18,19] Traction and

contraction forces exerted by the cytoskeleton are observed in viable cells. The termini of the cytoskeleton are connected with ECM receptors, such as integrins. These forces are able to detach deposited ECM such as fibronectin from the dish surfaces, which is why deposited ECM was recovered together with the cells (Fig. 3C).

One of the main functions of superficial cells in the urinary bladder urothelium of mammals is to maintain the blood–urine barrier. The impermeability of the barrier is due to apical membrane specialization, that is, plaques that consist of an asymmetric unit membrane, cerebroside content, and the presence of proteoglycans. In addition, impermeable tight junctions seal the membranes of neighboring superficial cells. Occludin is the integral membrane protein exclusively localized at tight junctions. The molecular mass of occludin is distributed from 62 and 82 kDa, and two or three bands of lowest molecular mass are predominant because of the phosphorylation. This multiple banding of occludin has been found in all species so far examined.[20] In the present study, scanning electron microscopy showed that fine structures of the urothelial cell sheet surfaces, microridge and microvilli, were morphologically destroyed by dispase treatment. Furthermore, immunoblotting revealed that occludin in the urothelial cell sheets recovered by the low-temperature treatment exhibited intact molecular weight and the typical multiple band pattern. Dispase treatment, however, fragmented occludin. Our previous study with keratinocytes revealed that dispase treatment disrupted E-cadherin and laminin 5, whereas these molecules remained intact in keratinocyte sheets harvested by reducing the temperature in PIPAAm-bonded dishes.[11] Sugasi *et al.*[16] also presented a similar morphology of urothelial cell sheet surfaces harvested by dispase.

Furthermore, we have developed two- and three-dimensional cell sheet manipulation techniques[10,11,21] facilitating fabrication of three-dimensional constructs from harvested cell sheets. For example, cardiac myocyte sheets harvested from bonded dishes were successfully layered, and electrical communications were established between the layered sheets *in vitro*.[21] These layered constructs, subcutaneously grafted into rats, exhibited electrical potentials and macroscopic synchronous beating for more than several months. Implant experiments involving harvested urothelial sheet grafting onto deepithelialized gastrointestinal tissue are ongoing.

In conclusion, we demonstrated successful harvesting of urothelial cell sheets from temperature-responsive culture dishes without the need for dispase. The harvested urothelial cell sheets exhibited differentiated morphology susceptible to dispase disruption. This method will be useful in advancing studies on urinary tract tissue engineering.

ACKNOWLEDGMENTS

Dr. T.T. Sun (New York University, New York, NY) kindly provided rabbit antiserum to total bovine uroplakins. We gratefully acknowledge Shigeru Nagai, M.Sc., for assisting with surgical procedures, and Shigeru Horita, Mayuko Kawashima, and Hideki Nakayama, who provided assistance and advice with electron microscopy findings. We thank Dr. David W. Grainger (Colorado State University, Ft. Collins, CO), who provided useful technical comments, and Ms. Barbara Levene, who provided English editing. The present work was supported by a Japan Society for the Promotion of Science, Grant-in-Aid for Scientific Research Category C (14571524). This work was performed at the Institute of Advanced Biomedical Engineering and Science, Tokyo Women's Medical University, Tokyo, Japan.

REFERENCES

1. Kropp, B.P., Rippy, M.K., Badylak, S.F., Adams, M.C., Keating, M.A., Rink, R.C., and Thor, K.B. Regenerative urinary bladder augmentation using small intestinal submucosa: Urodynamic and histopathologic assessment in long-term canine bladder augmentations. J. Urol. **155**, 2098, 1996.
2. Probst, M., Piechota, H.J., Dahiya, R., and Tanagho, E.A. Homologous bladder augmentation in dog with the bladder acellular matrix graft. BJU Int. **85**, 362, 2000.
3. Oberpenning, F., Meng, J., Yoo, J.J., and Atala, A. De novo reconstitution of a functional mammalian urinary bladder by tissue engineering. Nat. Biotechnol. **17**, 149, 1999.
4. Oesch, I. Neourothelium in bladder augmentation: An experimental study in rats. Eur. Urol. **14**, 328, 1988.
5. Niku, S.D., Scherz, H.C., Stein, P.C., and Parsons, C.L. Intestinal de-epithelialization and augmentation cystoplasty: An animal model. Urology **46**, 36, 1995.
6. Salle, J.L., Fraga, J.C., Lucib, A., Lampertz, M., Jobim, G., and Putten, A. Seromuscular enterocystoplasty in dogs. J. Urol. **144**, 454, 1990.
7. Motley, R.C., Montgomery, B.T., Zollman, P.E., Holley, K.E., and Kramer, S.A. Augmentation cystoplasty utilizing de-epithelialized sigmoid colon: A preliminary study. J. Urol. **143**, 1257, 1990.
8. Gonzalez, R., Buson, H., Reid, C., and Reinberg, Y. Seromuscular colocystoplasty lined with urothelium: Experience with 16 patients. Urology **45**, 124, 1995.
9. Aktug, T., Ozdemir, T., Agartan, C., Ozer, E., Olguner, M., and Akgur, F.M. Experimentally prefabricated bladder. J. Urol. **165**, 2055, 2001.
10. Kushida, A., Yamato, M., Kikuchi, A., and Okano, T. Two-dimensional manipulation of differentiated Madin-Darby canine kidney (MDCK) cell sheets: The noninvasive harvest from temperature-responsive culture dishes and transfer to other surfaces. J. Biomed. Mater. Res. **54**, 37, 2001.
11. Yamato, M., Utsumi, M., Kushida, A., Konno, C., Kikuchi, A., and Okano, T. Thermo-responsive culture dishes allow

the intact harvest of multilayered keratinocyte sheets without dispase by reducing temperature. Tissue Eng. **7**, 473, 2001.
12. Heskins, M., Guillent, J.E., and James, E. Solution properties of poly(*N*-isopropylacrylamide). J. Macromol. Sci. Chem. **A2**, 1441, 1968.
13. Fujiyama, C., Masaki, Z., and Sugihara, H. Reconstruction of the urinary bladder mucosa in three-dimensional collagen gel culture: Fibroblast–extracellular matrix interactions on the differentiation of transitional epithelial cells. J. Urol. **153**, 2060, 1995.
14. Hirose, M., Kwon, O.H., Yamato, M., Kikuchi, A., and Okano, T. Creation of designed shape cell sheets that are noninvasively harvested and moved onto another surface. Biomacromolecules **1**, 377, 2000.
15. Rheinwald, J.G., and Green, H. Serial cultivation of strains of human epidermal keratinocytes: The formation of keratinizing colonies from single cells. Cell **6**, 331, 1975.
16. Sugasi, S., Lesbros, Y., Bisson, I., Zhang, Y.Y., Kucera, P., and Frey, P. In vitro engineering of human stratified urothelium: Analysis of its morphology and function. J. Urol. **164**, 951, 2000.
17. Tash, J.A., David, S.G., Vaughan, E.E., and Herzlinger, D.A. Fibroblast growth factor-7 regulates stratification of the bladder urothelium. J. Urol. **166**, 2536, 2001.
18. Okano, T., Yamada, N., Okuhara, M., Sakai, H., and Sakurai, Y. Mechanism of cell detachment from temperature-modulated, hydrophilic–hydrophobic polymer surfaces. Biomaterials **16**, 297, 1995.
19. Yamato, M., Okuhara, M., Karikusa, F., Kikuchi, A., Sakurai, Y., and Okano, T. Signal transduction and cytoskeletal reorganization are required for cell detachment from cell culture surfaces grafted with a temperature-responsive polymer. J. Biomed. Mater. Res. **44**, 44, 1999.
20. Sakakibara, A., Furuse, M., Saitou, M., Ando-Akatsuka, Y., and Tsukita, S. Possible involvement of phosphorylation of occludin in tight junction formation. J. Cell Biol. **137**, 1393, 1997.
21. Shimizu, T., Yamato, M., Isoi, Y., Akutsu, T., Setomaru, T., Abe, K., Kikuchi, A., Umezu, M., and Okano, T. Fabrication of pulsatile cardiac tissue grafts using a novel 3-dimensional cell sheet manipulation technique and temperature-responsive cell culture surfaces. Circ. Res. **90**, e40, 2002.

Address reprint requests to:
Teruo Okano, Ph.D.
Institute of Advanced Biomedical Engineering and Science
Tokyo Women's Medical University
8-1 Kawada-Cho, Shinjuku-Ku, Tokyo 162-8666 Japan

E-mail: tokano@abmes.twmu.ac.jp

Young Investigator Award, 29th Annual Meeting of the Society for Biomaterials, Reno, NV, April 30–May 3, 2003

Nanofabrication for micropatterned cell arrays by combining electron beam-irradiated polymer grafting and localized laser ablation

Masayuki Yamato,[1] Chie Konno,[1] Shunsuke Koike,[2] Yuki Isoi,[1] Tatsuya Shimizu,[1] Akihiko Kikuchi,[1] Kimiko Makino,[2] Teruo Okano[1]

[1]*Institute of Advanced Biomedical Engineering and Technology, Tokyo Women's Medical University, Kawada-cho 8-1, Shinjuku-ku, Tokyo 162-8666, Japan*

[2]*Faculty of Pharmaceutical Sciences, Tokyo University of Science, 2641 Yamazaki Noda-shi, Chiba, 278-8510, Japan*

Received 15 October 2002; revised 6 February 2003; accepted 10 February 2003
Published online 30 October 2003 in Wiley InterScience (www.interscience.wiley.com). DOI: 10.1002/jbm.a.10078

Abstract: Most methods reported for cell-surface patterning are generally based on photolithography and use of silicon or glass substrates with processing analogous to semiconductor manufacturing. Herein, we report a novel method to prepare patterned plastic surfaces to achieve cell arrays by combining homogeneous polymer grafting by electron beam irradiation and localized laser ablation of the grafted polymer. Poly(*N*-isopropylacrylamide) (PIPAAm) was covalently grafted to surfaces of tissue culture-grade polystyrene dishes. Subsequent ultraviolet ArF excimer laser exposure to limited square areas (sides of 30 or 50 μm) produced patterned ablative photodecomposition of only the surface region (~100-nm depth). Three-dimensional surface profiles showed that these ablated surfaces were as smooth and flat as the original tissue culture-grade polystyrene surfaces. Time-of-flight secondary ion mass spectrometry analysis revealed that the ablated domains exposed basal polystyrene and were surrounded with PIPAAm-grafted chemistry. Before cell seeding, fibronectin was adsorbed selectively onto ablated domains at 20°C, a condition in which the non-ablated grafted PIPAAm matrix remains highly hydrated. Hepatocytes seeded specifically adhered onto the ablated domains adsorbed with fibronectin. Because PIPAAm inhibits cell adhesion and migration even at 37°C when the grafted density is >3 μg/cm^2, all the cells were confined within the ablated domains. A 100-cell domain array was achieved by this method. This surface modification technique can be utilized for fabrication of cell-based biosensors as well as tissue-engineered constructs.

J Biomed Mater Res 67A: 1065–1071, 2003

Key words: cell patterns; polymer grafting; *N*-isopropylacrylamide; laser ablation; cell culture; polystyrene; fibronectin

INTRODUCTION

Recently, surface patterning in cell culture has received significant attention for applications in biomaterials science because this technique is used for basic studies on surface chemistry, geometry,[1,2] and topographical[3,4] effects on cell behavior, cell–cell interactions,[5] as well as further applications to tissue engineering,[6] fabrication of novel biosensors, and bioassay devices incorporating cultured cells.[7] Several methods including photolithography,[5,8–12] microcontact printing,[13–16] microfluidics,[17–20] and use of elastomeric membranes having many holes[21,22] are reported to achieve micrometer-scale surface patterning. Although metals, silicon wafers, and glasses have frequently been used as materials subjected to lithographic patterning, few data are available for plastics typically used in bioassay and biotechnology devices.

Because the use of plastics simplifies fabrication and reduces costs for disposable cell-based biosensors and microelectromechanical systems,[23] we now demonstrate a novel method to pattern surfaces for convenient self-selective cell seeding and culture using combinations of polymer surface grafting and laser ablation. We have previously utilized electron beam (e-beam) irradiation for surface modification with polymers including a temperature-responsive polymer, poly(*N*-isopropylacrylamide) (PIPAAm),[24,25] and a non-cell adhesive polymer, poly(*N*,*N*′-dimethylac-

Correspondence to: M. Yamato; e-mail: myamato@abmes.twmu.ac.jp
Contract grant sponsor: Micromachine Center of Japan

rylamide).[26] Advantages of e-beam irradiation lie in its simple protocol for covalent polymer grafting. Only three steps are involved: spreading a dilute monomer solution on surfaces, e-beam irradiation, and subsequent washing. Although the grafted polymer thickness can be controlled by monomer concentration and radiation energy, it is limited by radical lifetime: a typical thickness obtained by PIPAAm grafting is <100 nm.

Using this technique, we have established a novel cell harvest method without use of trypsin or other proteolytic enzymes by utilizing thermo-responsive culture dishes on which PIPAAm was covalently grafted.[24] PIPAAm-grafted surfaces are relatively hydrophobic at 37°C, comparable to tissue culture polystyrene (TCPS) dishes, and become reversibly and highly hydrated below the grafted polymer lower critical solution temperature (LCST, 32°C).[24,27,28] Various cell types have been shown to adhere, spread, and proliferate on thermo-responsive culture dishes at 37°C, but spontaneously lift as contiguous cell sheets from these surfaces by simply reducing culture temperature below the grafted polymer LCST, 32°C.[29,30] Below the LCST, serum and matrix protein adsorption and cell adhesion are severely suppressed on the thermo-responsive culture dishes, similar to behavior on nonadhesive polyethyleneglycol-grafted dishes. E-beam radiation, easily masked by various materials including glass, metals, and plastics such as polyethylene, can also be used for patterned grafting of PIPAAm on culture surfaces, yielding localized thermo-responsive surface regions. These patterned surfaces are utilized for cell co-culture.[31] We have found that a higher density (beyond 3 μg/cm^2) of PIPAAm grafting inhibits cell adhesion even above the LCST.[32] In the present study, laser ablation, used previously for surface topographic modification,[33–35] is used for micropatterning of homogeneous PIPAAm-grafted culture dishes to achieve micropatterned cell seeding in arrays of regular and defined sizes.

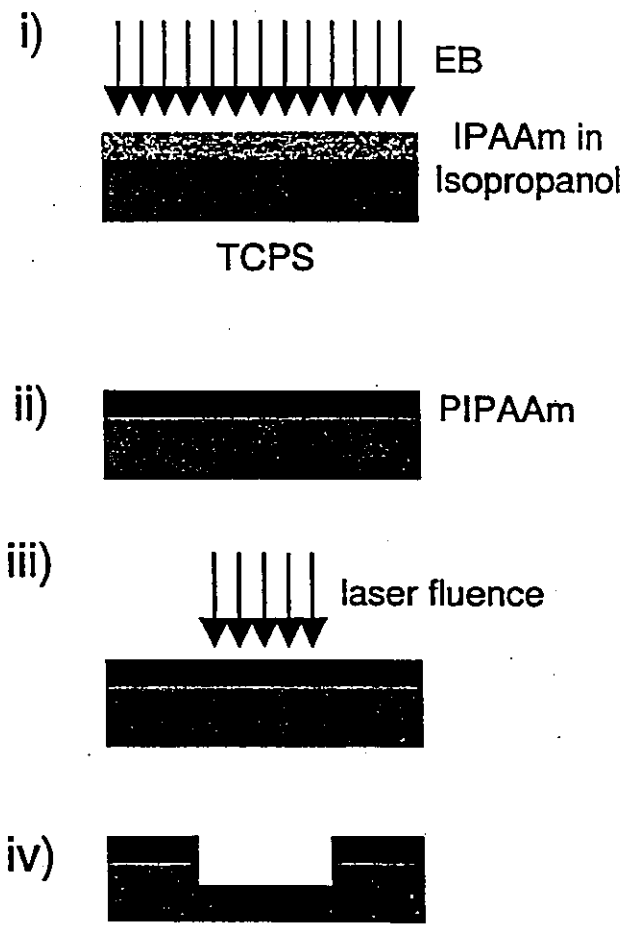

Figure 1. Schematic drawing of patterning on cell culture surfaces. Patterned surfaces were obtained by the combination of homogenous PIPAAm grafting by e-beam irradiation and laser ablation of selected domains. IPAAm monomer in isopropanol was spread onto TCPS and subjected to e-beam irradiation (i), producing PIPAAm covalently grafted across the entire TCPS surface (ii). Selected surface areas were subsequently irradiated with a UV excimer laser (iii), producing ablated domains re-exposing the basal TCPS substrate (iv).

MATERIALS AND METHODS

Covalent e-beam grafting of thermo-responsive polymer

PIPAAm was covalently grafted onto commercial TCPS dishes (Becton-Dickinson Falconware) using e-beam irradiation as described previously.[25] In brief, *N*-isopropylacrylamide monomer (IPAAm, Kohjin, Japan) was dissolved in 2-propanol at a concentration of 60 wt %. The solution (30 μL) was added and spread uniformly over each TCPS dish (35 mm in diameter), and subjected to irradiation with 0.3 MGy e-beam using an Area Beam Electron Processing System (Nisshin High Voltage, Japan). PIPAAm-grafted culture dishes were washed extensively with cold distilled water to remove ungrafted monomer. The presence of PIPAAm was confirmed by electron spectroscopy for chemical analysis (ESCA 750; Shimadzu, Kyoto, Japan). Homogeneity of PIPAAm grafting on TCPS surfaces was confirmed using field emission scanning electron microscopy. The amount of grafted PIPAAm was determined by attenuated total reflection Fourier transform infrared spectrophotometry. Because the base substrate comprises TCPS, absorption at 1600 cm^{-1} results from the TCPS monosubstituted aromatic ring. As PIPAAm was grafted onto the TCPS surface, strong amide absorption appeared in the region of 1650 cm^{-1}. The peak intensity ratio (I_{1650}/I_{1600}) was used to determine PIPAAm grafting density on the surface using the calibration curve of a known PIPAAm amount cast onto TCPS from solution. Grafted densities of PIPAAm used in the present study were estimated to be 3 μg/cm^2. Hepatocytes were not adherent on PIPAAm-grafted surfaces having this graft density at any culture temperature.

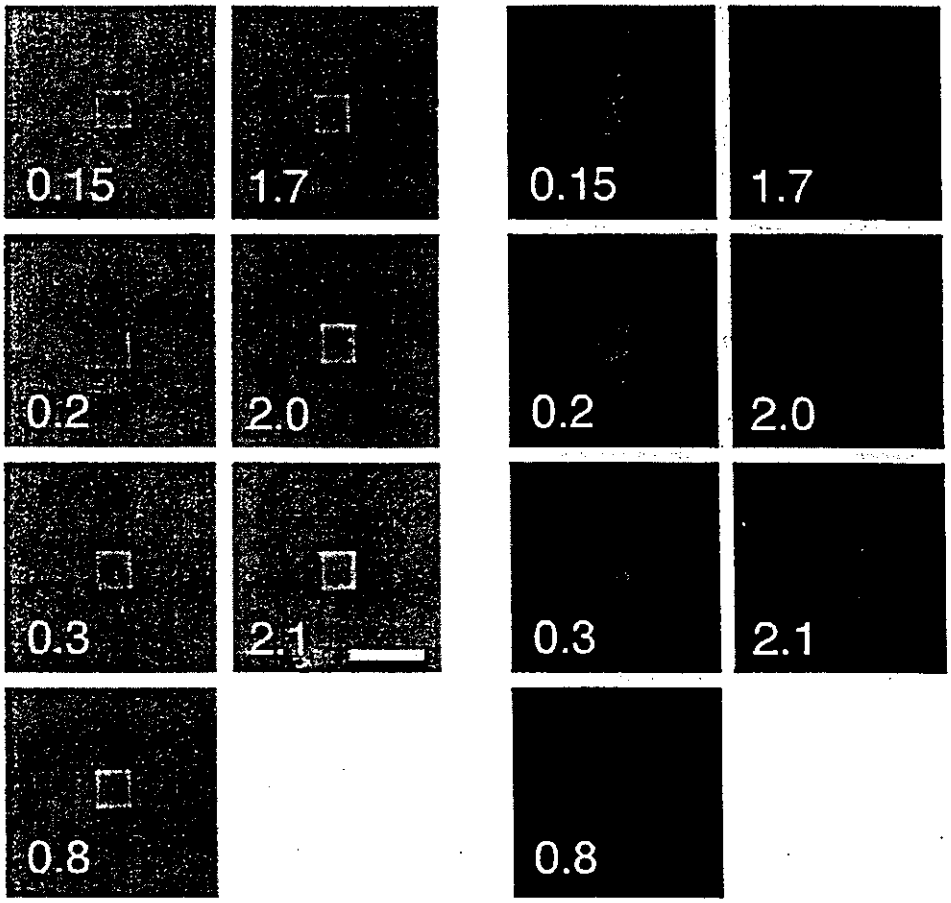

Figure 2. Effects of laser fluence on surface chemistry. PIPAAm-grafted surfaces irradiated with a UV excimer laser of various laser fluences (designated in each panel, J/cm^2) through a square hole pattern (30-μm sides) were examined by phase contrast microscopy or fluorescence microscopy after staining with a hydrophobic fluorescent dye. Scale bar = 100 μm. [Color figure can be viewed in the online issue, which is available at www.interscience.wiley.com.]

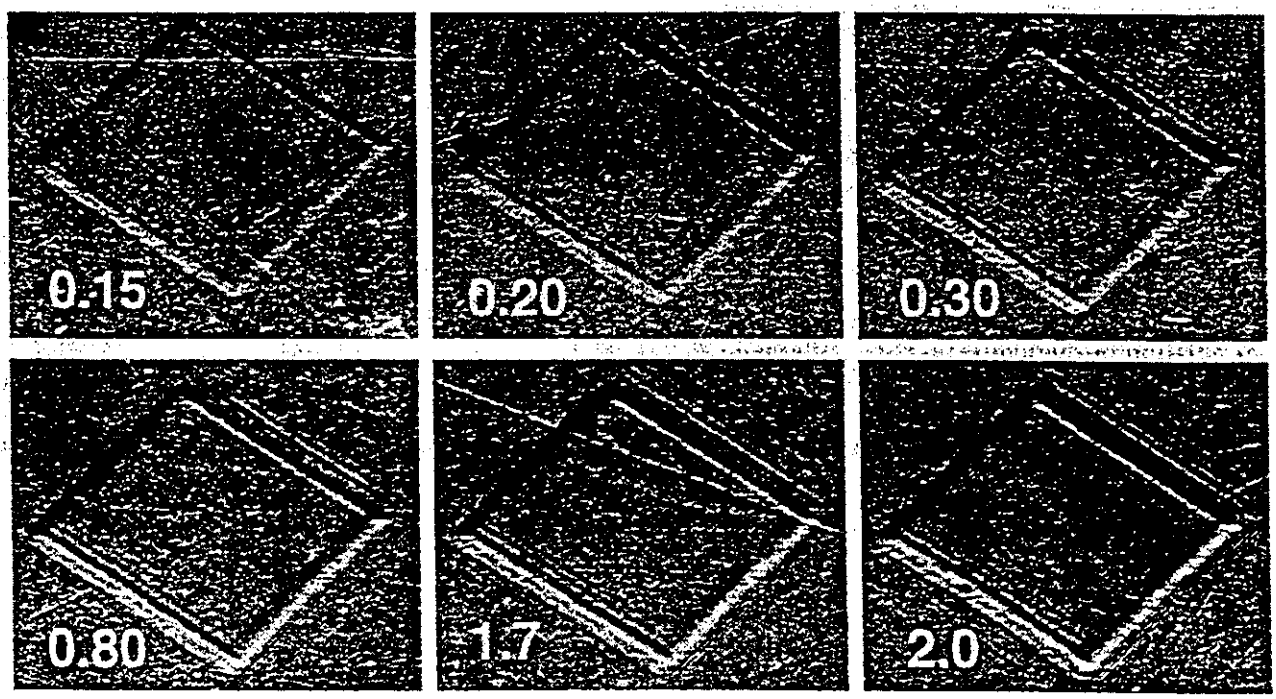

Figure 3. Scanning electron microscopy of laser ablated patterned surfaces. PIPAAm-grafted surfaces irradiated with a UV excimer laser of various laser fluences (designated in each panel, J/cm^2) through a square hole pattern (30-μm sides) were observed under a scanning electron microscope. Some image blur was observed outside the domains ablated with fluences of >0.3 J/cm^2.

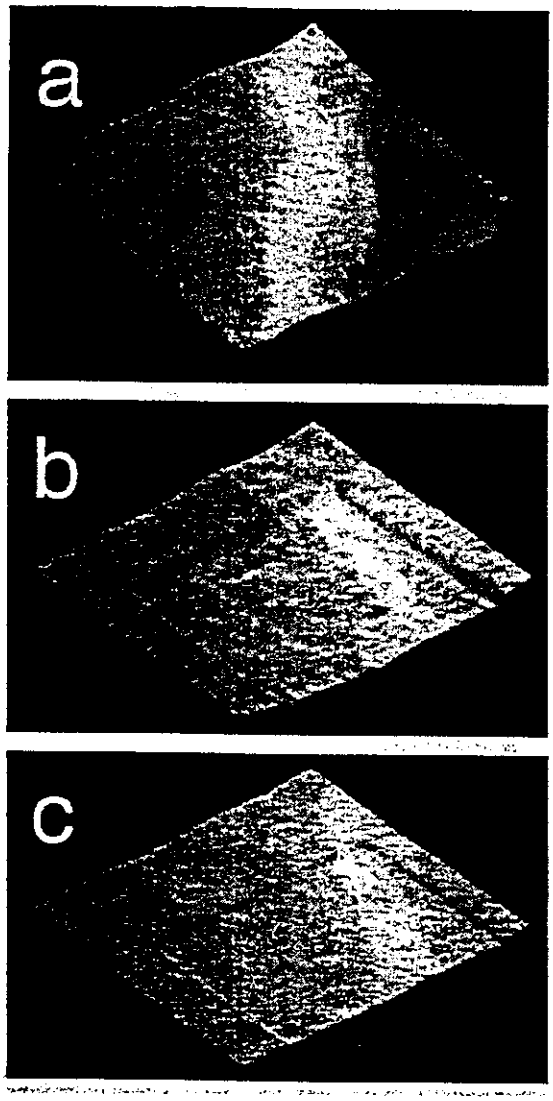

Figure 4. Three-dimensional profiles of laser ablated patterned surfaces. PIPAAm-grafted surfaces were irradiated with UV excimer laser through a square hole mask pattern with 100-μm sides, and observed by reflective confocal laser scanning microscopy. The applied laser fluence was 0.8 (b) and 0.2 J/cm^2 (c). Both ablated surfaces were as smooth and flat as the original TCPS surfaces (a). The depth of ablated regions was approximately 120 and 60 nm with 0.8 and 0.2 J/cm^2 laser ablation fluences, respectively.

Laser ablation of thermo-responsive patterned cell culture surfaces

Irradiation of culture dishes after PIPAAm was covalently grafted using an ArF excimer laser (wavelength 193 nm and pulse width 5 ns, L5910 III B; Hamamatsu Photonics, Japan) was achieved by passing a laser pulse through an optical microscope, resulting in ablative photodecomposition. The control unit was designed to control the fluence of the laser, pulse number, size of irradiated areas, and irradiation micropositioning. Laser ablative patterning utilized a square hole template whose sides were controlled in various size regimes. Ablated surfaces were observed by bright field, phase contrast, or reflective differential interference microscopy (Nikon, Tokyo, Japan), and the three-dimensional profiles were obtained by reflective confocal laser scanning microscopy (VK-8500; KEYENCE, Japan) immediately after ablation. The ablated surfaces were also examined under a S-800 scanning electron microscope (Hitachi, Tokyo, Japan).

Time-of-flight secondary ion mass spectrometry (TOF-SIMS)

To examine the presence or absence of PIPAAm, laser ablated surfaces were examined by TOF-SIMS (Tof-SIMS IV; Cameca Instruments, France). Secondary ions were collected and imaged in the gallium high-current bunched mode under the following instrumental conditions: field of view: 250 × 250 μm^2, 128 × 128 pixels, 512 shots per pixels; primary gallium ion beam: 25 keV, 1 pA; pulse width: <1 ns; primary dose density: 8.4 × 10^{12} cm^{-2}; image acquisition time: 14 min.

Visualization of patterned dish surfaces

Patterned dish surfaces were visualized using a hydrophobic cyanine dye, diIC18(3) (Molecular Probes) or bovine plasma fibronectin (FN; Nitta Gelatin, Japan) adsorbed from aqueous solution and immunostained *in situ*. DiIC18(3) has two long aliphatic hydrocarbon chains (C-18) that promote dye partitioning into hydrophobic domains. DiIC18 in Dulbecco's phosphate buffered saline (PBS) solution (25 μg/mL) was poured into the dishes and left for 100 min. After washing with PBS, the stained dishes were observed under the fluorescence microscope (Nikon). FN in PBS solution was plated on the dish at the concentration of 50 μg/mL and incubated at 20°C overnight. After washing with PBS, adsorbed FN was detected with anti-FN antibody (Biogenesis, UK) and fluorescein isothiocyanate-conjugated anti-rabbit immunoglobulin G antibody (Cappel Products, OH), and observed under a fluorescence microscope (Nikon).

Cells and cell culture

Rat primary hepatocytes were obtained as previously described using collagenase for cell dissociation.[25] The primary culture was plated on patterned surfaces, which were preincubated with 1 μg/mL FN in PBS for 2 h at 20°C, in Dulbecco's modified Eagle's medium supplemented with 10% fetal bovine serum, 100 units/mL penicillin, 100 μg/mL streptomycin, 10 ng/mL epidermal growth factor, 10 mmol/L nicotinamide, 0.2 mmol/L L-ascorbic acid 2-phosphate, and 1% dimethylsulfoxide.[36] Plated cells were incubated in a humidified atmosphere with 5% CO_2 at 20°C for 5 h. Unattached cells were then washed away, and the culture temperature was increased to 37°C. Cell morphology was monitored under a phase contrast microscope (ET300; Nikon).

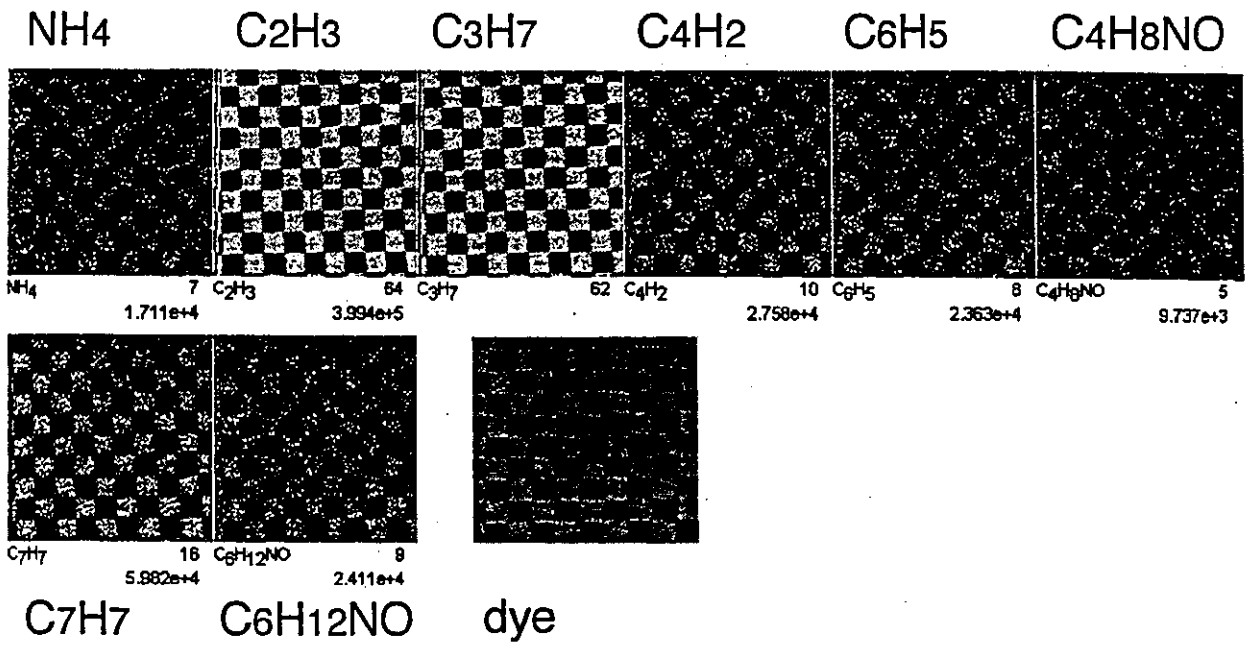

Figure 5. TOF-SIMS images of laser-ablated PIPAAm-grafted surfaces. PIPAAm-grafted surfaces were irradiated with 0.2 J/cm^2 laser fluence through a square hole mask pattern with 30-μm sides and examined by TOF-SIMS. Ablated domains were arrayed checkerwise and separated by 30 μm. The fluorescence microscopic image obtained after hydrophobic dye staining is also shown. [Color figure can be viewed in the online issue, which is available at www.interscience.wiley.com.]

RESULTS

Surface micropatterning was achieved by the combination of homogeneous PIPAAm grafting using e-beam irradiation and laser ablation of limited selected areas (Fig. 1). Ablated surfaces were examined by several different microscopy methods. Whereas ablated areas were not detected by simple bright field microscopy, patterned domain edges were clearly detected by phase contrast or reflective differential interference microscopy (Fig. 2, left panel), suggesting that edge contrast is sharp. Scanning electron microscopy revealed that whereas some image blurring was observed outside domains ablated with the laser fluence of >0.3 J/cm^2, these effects were not detected in samples ablated with a fluence of <0.2 J/cm^2 (Fig. 3). Square laser ablated domains were detected under a phase contrast or a scanning electron microscope, but chemical modification by higher laser fluence was revealed by fluorescence microscopy after staining with hydrophobic fluorescent dye (Fig. 2, right panel). Lower laser fluence (<0.2 J/cm^2) resulted in square stained domains corresponding with domains detected by phase contrast microscopy implying re-exposure of the hydrophobic polystyrene base, but higher laser fluence damaged the chemistry. To obtain a more accurate surface profile, ablated surfaces were examined by reflective confocal laser scanning microscopy (Fig. 4). The ablated surfaces appeared as smooth and flat as the original TCPS surfaces before ablation. Depth of ablated domains was approximately 60 and 120 nm with 0.2 and 0.8 J/cm^2 laser ablation fluences, respectively.

Surfaces patterned checkerwise by 0.2 J/cm^2 laser ablation were examined by TOF-SIMS (Fig. 5), and compared with similar surfaces stained with a hydrophobic dye (*dye* in Fig. 5). These images provide detailed information about the lateral distribution of the secondary ion emission and, hence, also the corresponding surface-derived species. Secondary ions containing nitrogen and/or oxygen atoms attributed only to PIPAAm were detected only on non-ablated regions (designated in red in Fig. 5), whereas secondary ions attributed to polystyrene were detected only on ablated domains (designated in blue in Fig. 5). Thus, these TOF-SIMS imaging data support complete ablative removal of the grafted PIPAAm in the selected patterned regions. Resulting hydrophobicity changes caused by ablation of grafted PIPAAm were also shown by FN adsorption below the LCST where PIPAAm is highly hydrated and FN adsorption on this chemistry is selectively suppressed [Fig. 6(a), left]. Adsorbed FN was detected only on the laser-ablated domains where PIPAAm is removed as shown by TOF-SIMS images. Pattern fidelity is maintained by selective FN adsorption to exposed TCPS. Additionally, cell adhesion results support this selective FN deposition. Rat primary hepatocytes were seeded onto the patterned surfaces preadsorbed with 1 μg/mL FN at 20°C for 2 h and cultured at 20°C for 5 h, a condition in which PIPAAm surface chemistry is hydrated and nonadhesive to proteins and cells.[31] After washing away unattached cells, culture temperature was increased to 37°C to collapse the PIPAAm chemistry. Hepatocytes adhered specifically onto the laser-ablated domains lacking PIPAAm chemistry and were

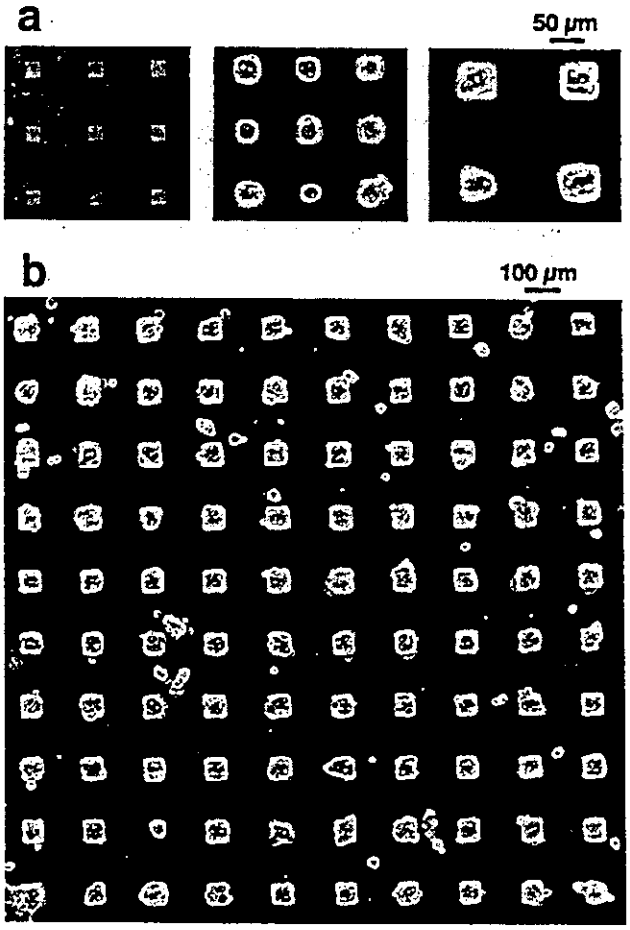

Figure 6. Microphotographs of obtained hepatocyte-cultured arrays. PIPAAm-grafted surfaces were irradiated with 0.2 J/cm^2 laser fluence through a square hole pattern with 30 [left and center in image (a)], or 50-μm sides [right in images (a), and (b)], and challenged with FN solution adsorption below the LCST of PIPAAm [left in (a)] and hepatocyte seeding [center and right in (a) and (b)]. Pattern fidelity with cells is highly preserved because of the selective FN deposition into the ablated areas of exposed TCPS. Photomicrographs were taken after 4-day culture. See text for further details. [Color figure can be viewed in the online issue, which is available at www.interscience.wiley.com.]

thus spontaneously arrayed into these patterned areas. All the domains were occupied by cells. Each ablated domain with sides of 30 μm was occupied with a single hepatocyte [Fig. 6(a), center], whereas two or three hepatocytes shared each of the ablated domains with sides of 50 μm [Figs. 6(a), right or 6(b)]. These cell array patterns were maintained for >2 weeks, because high grafting density of the surrounding PIPAAm matrix inhibited hepatocyte outgrowth from the ablated adhesive domains.

DISCUSSION

In the present study, the grafted PIPAAm polymer density was experimentally determined to be 3 μg/cm^2. Considering a typical bulk polymer density to be approximately 1 g/cm^3, grafted PIPAAm thickness therefore approximates 30 nm. Because the laser-ablated depth is shown here to exceed this thickness, the grafted thin PIPAAm layer should be completely removed, exposing the basal TCPS in these patterned regions. This is confirmed by four experimental findings correlated to pattern fidelity: hydrophobic dye staining, TOF-SIMS, FN adsorption, and cell adhesion. Because the ablated depth was much smaller than the typical dimensions of ~500 nm needed for cell attachment, spreading, and alignment responses on grooved surfaces,[4] the observed cell adhesion specific to ablated areas is proposed to result from differences in surface hydrophobicity between PIPAAm-grafted and ablated domains that facilitate surface-selective deposition of the cell adhesion protein, FN.[37]

Previously, excimer lasers have been used for the preparation of patterned surfaces.[38] In that study, a thin polymer layer was prepared on a polymer substrate by a laser-induced forward transfer technique. This method requires solvent casting of a polymer on a polymeric substrate as well as washing of the ungrafted polymer after irradiation, or mechanical pressing of a polymer film to a substrate to make polymer bilayers before laser irradiation. This technique limits the combinations of polymer types for bilayering and is applicable only to combinations of ultraviolet (UV)-transparent substrate polymers and grafted polymers having relatively large UV absorption coefficients. By separating the grafting and patterning steps, such a limitation is excluded in the present method. Self-assembled monolayers (SAMs) have also exploited laser ablative patterning because thin metallic films such as Au deposited on glass are easily desorbed by UV irradiation.[39] Drawbacks associated with the SAM strategy include stability problems associated with anchor oxidation under both ablative and cell culture conditions, the necessity to use specific metal substrates, and the limited film thickness introduced onto surfaces. For example, the PIPAAm layer of 30-nm thickness obtained by e-beam irradiation in the present study cannot be achieved using SAM techniques.

We conclude that this surface modification method combining polymer grafting by e-beam irradiation with limited laser ablation has the advantages of broad substrate applicability, high pattern fidelity, and reduced fabrication costs to produce miniaturized cell-based devices relevant for high-speed biomolecule analysis, for disease diagnosis, as well as tissue engineering.

The authors are thankful to Professor David W. Grainger, Colorado State University, for his valuable comments.